Cancer Immunology, Immunotherapy (2019) 68:489–502
https://doi.org/10.1007/s00262-019-02301-3

ORIGINAL ARTICLE

STAT3 inhibition specifically in human monocytes and macrophages by CD163-targeted corosolic acid-containing liposomes

Morten Nørgaard Andersen[1,2,3] · Anders Etzerodt[2] · Jonas H. Graversen[4] · Lisa C. Holthof[5] · Søren K. Moestrup[1,2,4] · Marianne Hokland[2] · Holger J. Møller[1]

Received: 30 August 2018 / Accepted: 6 January 2019 / Published online: 14 January 2019

Abstract

Tumor-associated macrophages (TAMs) are of major importance in cancer-related immune suppression, and tumor infiltration by CD163^{pos} TAMs is associated with poor outcome in most human cancers. Therefore, therapeutic strategies for reprogramming TAMs from a tumor-supporting (M2-like) phenotype towards a tumoricidal (M1-like) phenotype are of great interest. Activation of the transcription factor STAT3 within the tumor microenvironment is associated with worse prognosis, and STAT3 activation promotes the immunosuppressive phenotype of TAMs. Therefore, we aimed to develop a drug for inhibition of STAT3 specifically within human TAMs by targeting the endocytic CD163 scavenger receptor, which is highly expressed on TAMs. Here, we report the first data on a CD163-targeted STAT3-inhibitory drug consisting of corosolic acid (CA) packaged within long-circulating liposomes (LCLs), which are CD163-targeted by modification with monoclonal anti-CD163 antibodies (αCD163)—CA-LCL-αCD163. We show, that activation of STAT3 (by phosphorylation) was inhibited by CA-LCL-αCD163 specifically within CD163^{pos} cells, with minor effect on CD163^{neg} cells. Furthermore, CA-LCL-αCD163 inhibited STAT3-regulated gene expression of IL-10, and increased expression of TNFα, thus indicating a pro-inflammatory effect of the drug on human macrophages. This M1-like reprogramming at the mRNA level was confirmed by significantly elevated levels of pro-inflammatory cytokines (IFNγ, IL-12, TNFα, IL-2) in the culture medium. Since liposomes are attractive vehicles for novel anti-cancer drugs, and since direct TAM-targeting may decrease adverse effects of systemic inhibition of STAT3, the present results encourage future investigation of CA-LCL-αCD163 in the in vivo setting.

Keywords Cancer · Signal transducer and activator of transcription 3 (STAT3) · Tumor-associated macrophage (TAM) · CD163 · Drug delivery

Abbreviations

CA	Corosolic acid
EPR effect	Enhanced permeability and retention effect
LCL	Long-circulating liposome
MDMs	Monocyte-derived macrophages
MFI	Median fluorescence intensity
PEG	Polyethylene glycol
pSTAT3	P-(Y705)-STAT3:activated STAT3 by Tyr-705-phosphorylation
STAT3	Signal transducer and activator of transcription 3
TAMs	Tumor-associated macrophages
UT	Untreated sample

Electronic supplementary material The online version of this article (https://doi.org/10.1007/s00262-019-02301-3) contains supplementary material, which is available to authorized users.

✉ Morten Nørgaard Andersen
morten@biomed.au.dk

[1] Department of Clinical Biochemistry, Aarhus University Hospital, Palle Juul-Jensen Boulevard 99, 8200 Aarhus N, Denmark

[2] Department of Biomedicine, Aarhus University, Aarhus, Denmark

[3] Department of Hematology, Aarhus University Hospital, Aarhus, Denmark

[4] Department of Molecular Medicine, University of Southern Denmark, Odense, Denmark

[5] Department of Hematology, Amsterdam UMC, VU University Medical Center, Cancer Center Amsterdam, Amsterdam, The Netherlands

Introduction

Extensive investigation has established the essential role of immune cells in development and progression of malignant diseases. Consequently, "tumor promoting inflammation" along with "tumor immune avoidance" are now considered hallmarks of cancer [1]. This has paved the way for novel immunomodulatory anti-cancer treatments that have shown favourable results in the clinical setting [2].

Tumor-associated macrophages (TAMs) are of major importance in establishing a tumor microenvironment that promotes tumor growth, angiogenesis, resistance to anti-tumor immunity and chemotherapy, and ultimately metastasis [3, 4]. This is reflected by results showing that high TAM-infiltration is associated with poor outcome in the majority of human malignancies [5–7]. In general, the TAM phenotype is anti-inflammatory (so-called M2-like) in contrast to pro-inflammatory and potentially tumoricidal macrophages (so-called M1-like) [3, 8, 9]. Interestingly, pro-inflammatory stimuli can reprogram TAMs from a tumor-promoting M2-like phenotype, towards tumoricidal M1-like cells [8, 10, 11]. Hence, TAMs are proposed as highly attractive targets for novel immunomodulatory anti-cancer therapy [4, 7, 12]. The first studies pursuing this goal focused on colony-stimulating factor 1 (CSF-1) inhibition, which has shown promising results in preclinical studies [13, 14]. However, clinical data have so far indicated limited effect on outcome, but trials are ongoing [15, 16]. Notably, the main rationale for using CSF-1 inhibitors was depletion of tumor-promoting TAMs [16]. Yet, a potentially more effective strategy could be reprogramming of TAMs from tumor promoting (M2-like) to a tumoricidal (M1-like) phenotype [4, 12, 16]. Such reprograming may be obtained by inhibition of the transcription factor signal transducer and activator of transcription 3 (STAT3) within TAMs [17–20].

STAT3 activation is increased in several human cancers (e.g. colorectal, gastric, hepatocellular, and ovarian carcinomas) [18, 21, 22], which was associated with immune suppression, as well as tumor cell proliferation, survival, and invasion [17, 18]. Indeed, studies using different approaches for inhibition of STAT3 (gene knockout, RNAi, or small molecule inhibitors) within immune cells (especially myeloid cells) have shown promising results in murine models. Notably, STAT3 inhibition increased IL-12 and TNFα production whereas it decreased IL-10 production, and induced M1-like reprogramming of murine macrophages [23–25]. Ablation of STAT3 in mice, either within the hematopoietic compartment, or within myeloid and B cells, induced potent anti-tumor immunity [26, 27]. Interestingly, recent data showed that STAT3-ablation specifically within CD68 expressing TAMs inhibited tumor growth, angiogenesis, and metastasis, and prolonged survival in a mouse model of breast cancer [28]. Another paper showed activation of STAT3 in $CD163^{pos}$ TAMs within human tumors, and that anti-tumor effects of ERK5 inhibition were mediated by inhibition of STAT3 [29].

The hemoglobin–haptoglobin scavenger receptor CD163 is among the most well-described markers of M2-polarized macrophages, and especially TAMs [9, 30, 31]. Indeed, infiltration by $CD163^{pos}$ TAMs is associated with poor outcome in several human cancers [5, 31–33]. CD163 and the anti-inflammatory cytokine IL-10 are both markers of M2-polarized macrophages (including TAMs), and may be upregulated in vitro by tumor cell supernatant or IL-10 itself via activation of STAT3 [34–36]. Importantly, corosolic acid (CA), a STAT3-inhibitory natural compound inhibited such M2-like polarization of human macrophages [37]. Further, in vivo experiments showed anti-tumor effects of CA in a murine osteosarcoma model, likely owing to activation of anti-tumor immunity [38].

Since CD163 is an endocytic receptor with high expression on TAMs, it may be an ideal gateway for delivery of anti-cancer therapeutics. Recently, we developed an antibody/liposome-based system that allows effective targeting of compounds to CD163-expressing cells [39]. Liposomes are attractive carriers for delivery of anti-cancer drugs to tumor tissues, owing to increased circulation time and passive accumulation of liposomes in tumors by the "enhanced permeability and retention" (EPR) effect (tumor blood vessels are leaky and lymphatic vessels less functional) leading to passive accumulation of liposomes in vivo [40, 41].

Thus, a CD163-targeted STAT3 inhibitor may be a novel effective and specific anti-cancer drug, as it may activate anti-tumor immunity by reprogramming TAMs. Consequently, we aimed to develop a liposome-based STAT3-inhibitory drug targeting human $CD163^{pos}$ cells (including TAMs).

Materials and methods

Production of long-circulating liposomes

Long-circulating liposomes (LCLs) containing 300 mM of calcium acetate were produced, and subsequently remote-loaded with corosolic acid.

The LCLs were prepared using a mixture of hydrogenated soy L-α phosphatidylcholine (HSPC), cholesterol, and 1,2-distearoyl-phosphoethanolamine-*N*-[methoxy(polyethylene glycol)-2000] (mPEG2000-DSPE) in molar ratio 55:40:5 (all from Avanti Polar Lipids, Alabaster, AL). Lipids were dissolved in methanol. To form calcium acetate-containing LCLs, lipids and 300 mM calcium

acetate buffer (at 70 °C) were run on the NanoAssemblr Platform (Precision Nanosystems, Vancouver, BC) with lipid:buffer flow rate ratio of 1:6. Alternatively, liposomes were produced by drop-wise addition of lipids (in ethanol) to 300 mM calcium acetate buffer (at 70 °C) and then sizing liposomes by extrusion 25 times through a 0.1 µm filter on an Avanti mini-Extruder (Avanti Polar Lipids). After production, liposomes were dialysed twice against isotonic saline.

For remote loading [42] of the produced LCLs, a solution of corosolic acid (CA, Sigma-Aldrich, Munich, Germany) in PBS with 1% DMSO was made. This was mixed with LCL suspension in a buffer with 35 mM citric acid and 0.85 mM CA and incubated for 60 min at 65 °C in a shaker incubator. After this incubation, the solution containing LCLs was transferred to micro-centrifuge tubes, and centrifuged for 5 min at 400*g* to remove excess CA.

To target CA-loaded LCLs (CA-LCLs) to the CD163 scavenger receptor, CA-LCLs were modified by insertion of a lipidated anti-human CD163 antibody into the CA-LCLs (αCD163, clone KN2/NRY, humanised IgG4 [43] was a gift from Affinicon ApS, Aarhus, Denmark). KN2/NRY insertion was done by PEGylation of the antibodies using 4-nitrophenol-coupled PEG3400 that was also coupled with the phospholipid DSPE to facilitate passive insertion into the liposome lipid bilayer, as described in more detail in [39]. After this modification, CA-LCLs without antibody as well as KN2/NRY-modified CA-LCLs (CA-LCL-αCD163) were dialysed twice (300 kDa cut off, Float-A-Lyzer, Spectrum Labs, Breda, Netherlands) against isotonic PBS, and were then sterile-filtered (0.2 µm) and stored at 4 °C.

Liposomes containing the green fluorescent dye calcein were made as described above for calcium acetate-LCLs using the NanoAssemblr, replacing the calcium acetate solution with an aqueous solution containing 200 mM calcein (Sigma-Aldrich).

Liposome size assessment was performed using dynamic light scatter measurements on a DynaPro NanoStar system (Wyatt Technology Europe GmbH, Dernbach, Germany), using Dynamics software 7.1.9 (Wyatt Technology Europe GmbH). Concentrations of lipid and CA were measured using high-pressure size-exclusion chromatography on a Dioxnex Ultimate 3000 HPLC system with UV-detection at 205 nm (GE Healthcare, Brøndby, Denmark).

Purification of peripheral blood mononuclear cells (PBMCs)

Human PBMCs were purified from buffy coats obtained from the blood bank, Department of Clinical Immunology, Aarhus University Hospital, Aarhus, Denmark. The PBMC fraction was purified by density-gradient centrifugation (400*g*, 30 min) on a Histoqaque-1077 gradient (Sigma-Aldrich) according to the manufacturer's instructions. After purification and wash in PBS/2% foetal calf serum (FCS), PBMCs were frozen at − 80 °C in RPMI-1640 medium with 20% FCS and 100 U/100 µg/mL penicillin/streptomycin (all from Lonza, Basel, Switzerland) and 10% DMSO (Sigma-Aldrich), or were used in experiments immediately. When PBMCs were used to purify $CD14^{pos}$ monocytes for culture of human monocyte-derived macrophages, the cells were not frozen before this purification step.

Culture of human monocyte-derived macrophages (MDMs)

Human MDMs were cultured from monocytes purified from PBMCs by EasySep™ human CD14-positive selection kit (StemCell Technologies, Cambridge, UK), according to the manufacturer's instructions. After isolation and wash, monocytes were cultured for 5–6 days in RPMI-1640 medium with 10% FCS, 100 U/100 µg/mL pen/strep, 10 ng/mL M-CSF, and 1 ng/mL GM-CSF (both from PeproTech, Hamburg, Germany) to induce differentiation into MDMs. For CD163-targeting experiments, cells were then stimulated with IL-10 (20 ng/mL, PeproTech) for 2–3 days to induce CD163 expression in MDMs. For harvesting adherent MDMs, cells were first loosened by 10–15 min incubation with PBS/0.5% bovine serum albumin (BSA)/5 mM EDTA/4 mg/mL Lidocaine (all from Sigma-Aldrich). Cells were then detached by pipetting and/or by scraping with a cell scraper.

Flow cytometry and confocal microscopy

All antibody stainings for flow cytometry were performed in 50–100 µL stain buffer (PBS/0.5%BSA/0.09%NaN_3) at 4 °C in the dark for 30 min, followed by washing with stain buffer. Less than 10^6 cells were added to each tube. The fluorochrome-conjugated monoclonal mouse-anti-human antibodies used were: anti-CD163 FITC (clone Mac2-158, Trillium Diagnostics, Bangor, ME), anti-CD163 PE (clone Mac2-158, Trillium Diagnostics), anti-CD11b BV510 (clone ICRF44, BD Biosciences, Erembodegem, Belgium), anti-CD45 AF700 (clone HI30, BD Biosciences), anti-P-Y705-STAT3 PE (pSTAT3, clone 4/P-STAT3, BD Biosciences). Blocking of non-specific staining was done with Human BD Fc Block™ (BD Biosciences) [44]. Dead cells were excluded by staining with Live/dead fixable dye near-IR (Life Technologies, Carlsbad, CA). Reagents were titrated for optimal performance. All fluorescence intensities are given as median values (MFI).

To perform intracellular staining for detection of pSTAT3, cells were fixed with 4% formaldehyde (Sigma-Aldrich) for 15 min/RT, washed and then permeabilized with 90% methanol (Sigma-Aldrich) 30 min/on ice. The cells were stained

with Live/dead near-IR viability dye before fixation with formaldehyde.

To validate our assay for detection of pSTAT3 by flow cytometry we performed a cross validation by western blot using another antibody clone for detection of pSTAT3 (Supplemental Fig. 1), showing concordant results.

Compensation of spectral overlap in flow cytometry experiments was done using single-stained antibody capture beads; BD™ Comp Beads Plus (BD Biosciences), OneComp eBeads™ (eBioscience, San Diego, CA), and ArC™ Comp beads for Live/dead (Thermo Fisher Scientific). All flow cytometry data were acquired on an LSR Fortessa flow cytometer (BD Biosciences). Data were analysed using FlowJo 10.0.7 for Mac (FlowJo, LLC, Ashland, OR). Gating in flow cytometry experiments was done based on unstained samples (Live/dead only), internal negatives (negative cells within the sample), as well as samples without cytokine stimulation. Gating strategies used are shown in Supplemental Fig. 2.

For confocal microscopy, MDMs were cultured on coverslips in 48-well plates. After treatment, medium was removed, wells were washed, and cells were fixated with 2% formaldehyde. Coverslips were then stained with DAPI fluorescent DNA stain (Thermo Fisher Scientific) 1 h at RT, and mounted on glass slides using Prolong Diamond mounting medium (Life Technologies). Confocal images were acquired using an LSM 710 confocal microscope (Carl Zeiss, Munich, Germany).

Cell toxicity assay

Human MDMs were plated in 96-well plates, and rested to allow attachment. Drugs (free CA, CA-LCL, or CA-LCL-αCD163) were added in stated final concentrations of CA. Medium (UT), or medium with relevant concentrations of DMSO served as controls. After 12 or 24 h incubation at 37 °C cell viability was assessed using CellTiter-Glo® luminescence assay (Promega Corporation, Madison, WI) according to the manufacturer's instructions. Luminescence signals were read on a GloMax Discover Microplate Reader (Promega).

Gene expression analysis by quantitative polymerase chain reaction (qPCR)

Cultured human MDMs were dissolved in RLT buffer and RNA was purified using the RNeasy mini kit (Qiagen, Hilden, Germany). Purified RNA was reverse-transcribed to cDNA in a reaction with 2.5 U/μL MulV reverse transcriptase enzyme (Applied Biosystems, Thermo Fisher Scientific Inc., Waltham, MA), 1.0 U/μL RNase inhibitors (Applied Biosystems), 1.0 mM dNTP mix (VWR International, Radnor, PA), 2.5 μM Oligo(dT) (DNA Technology, Risskov, Denmark), 1 × PCR buffer and 6.25 mM $MgCl_2$ (from Applied Biosystems). RNA input was 100 ng in a 20 μL reaction (RNA concentrations were measured using a NanoDrop 2000 spectrophotometer, Thermo Fisher Scientific).

Quantitative PCR was performed using a LightCycler 480 instrument (Roche, Basel, Switzerland) in a 10 μL reaction with 1 μL cDNA, primers, and 480 SYBR Green I Master mix (Roche) according to the manufacturer's instructions. Samples were run in duplicates. A standard curve was included in all runs, and was used to calculate relative concentrations of target mRNA. All qPCR results on human MDMs were normalized to the levels of GAPDH (housekeeping gene). Primers were purchased from Eurofins Genomics (Ebersberg, Germany). See Supplemental table 1 for primer sequences.

Measurement of pro-inflammatory cytokines within culture medium/supernatant

Using electro-chemo-luminescence-based multiplex sandwich immunoassays we measured levels of IFNγ, TNFα, IL-2, and IL-12 according to the manufacturer's instructions (Human Pro-inflammatory panel, Meso Scale Discovery, Rockville, MD). All medium samples were diluted 1:2 in assay dilution buffer.

Statistical analyses

Statistical analyses and figures were made using STATA version 14 for Mac (StataCorp LP, TX) and Prism 5d for Mac (GraphPad software, Inc., La Jolla, CA). Data are displayed as mean with standard error. To evaluate the effect of different CA formulations and concentrations, we used two-way mixed-effects ANOVA with relevant post-tests. *T* tests were used to evaluate statistical difference between two groups. A P value ≤ 0.05 was considered statistically significant.

Results

Characteristics and stability of corosolic acid-containing long-circulating liposomes

CA-LCLs were produced by remote loading of CA into LCLs as described. Figure 1a shows a schematic drawing of CA-LCL-αCD163, and the CA molecular structure.

The remote loading procedure was optimized by titration of the CA:cholesterol molar ratio and incubation time at 65 °C, identifying 1:10 molar ratio and 60 min as optimal (Fig. 1b).

Resulting LCLs had a mean radius ± (SD) of 56.2 nm (5.0) for non-modified CA-LCLs, and 62.0 nm (5.4) for

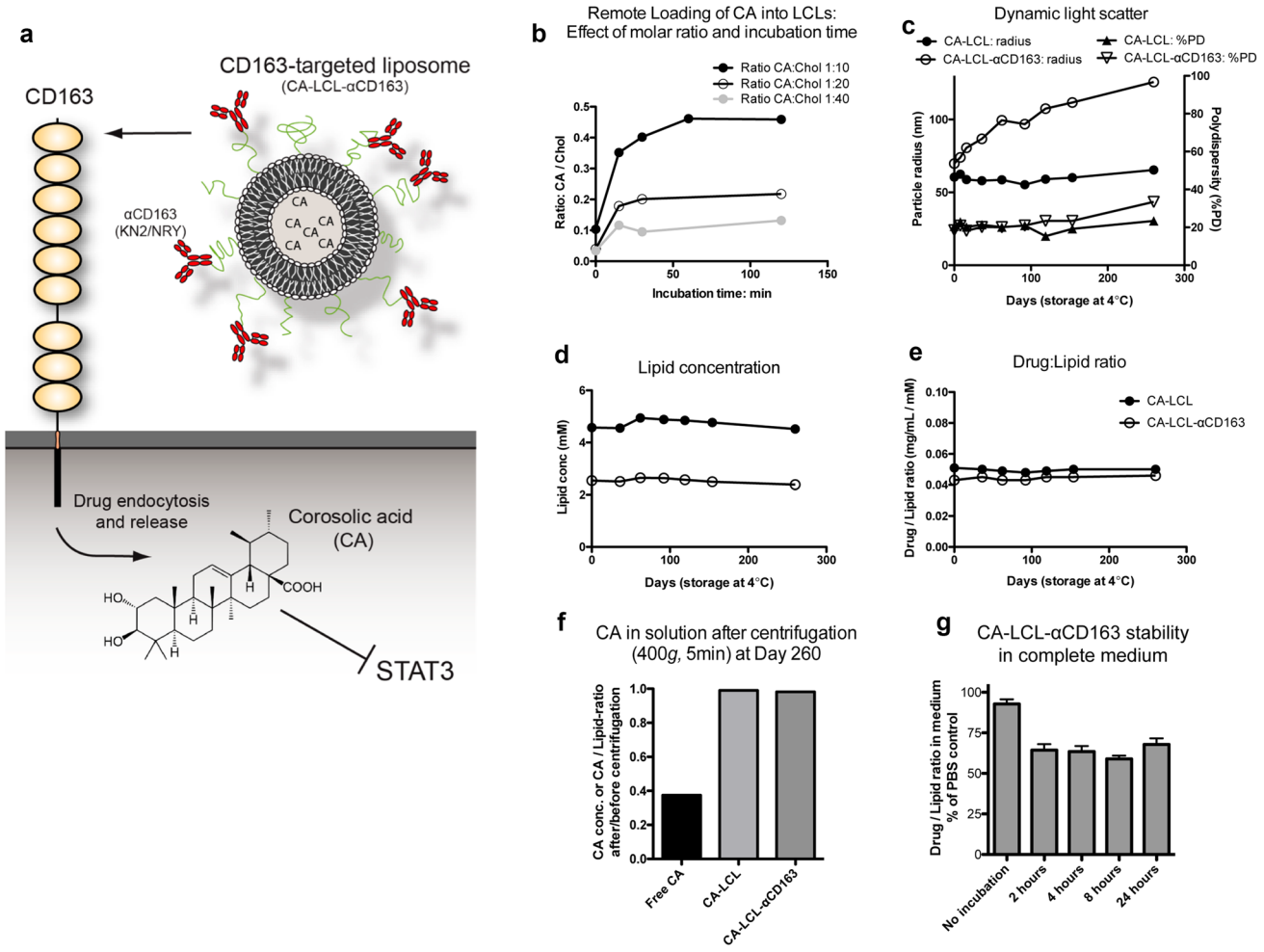

Fig. 1 CD163-targeted corosolic acid-containing long-circulating liposomes (CA-LCL-αCD163): remote loading of CA into LCLs and stability during storage. **a** Schematic drawing of a "long-circulating liposome" (LCL) containing corosolic acid (CA-LCL). The liposomes are targeted to the CD163 scavenger receptor by anti-CD163 antibodies (αCD163, KN2/NRY). Concentrations of CA (drug) and cholesterol (lipid) were measured by HPLC, and mean particle radius determined by dynamic light scatter measurements. **b** Various molar ratios of drug:lipid and various incubation times for remote loading of CA into LCLs (at 65 °C) showed that 1:10 molar ratio/60 min produced the highest drug:lipid ratio, and was used in subsequent production of CA-LCLs. **c** For CA-LCLs (non-modified) both the mean particle radius and polydispersity (size heterogeneity, %PD) were stable during storage at 4 °C, whereas for CA-LCL-αCD163 some increase in particle radius and slight increase in polydispersity was observed. **d, e** Lipid concentrations and drug:lipid ratios were largely unchanged during storage for > 8 months. After ultracentrifugation of CA-LCL and CA-LCL-αCD163 samples, no CA was detectable in the supernatants. **f** After slow centrifugation (400*g*/5 min) drug:lipid ratio was unchanged for CA-LCLs and CA-LCL-αCD163, whereas free CA was pelleted (due to low solubility in PBS), showing that CA did not leak from the liposomes—even after 8 months storage at 4 °C. **g** CA-LCL-αCD163 (30 μM CA) stability in complete medium with 10% calf serum at 37 °C. Drug:lipid ratio decreased ~ 32% during the first 2 h incubation, and thereafter remained stable

CA-LCL-αCD163. Figure 1c–e shows stability data for CA-LCLs and CA-LCL-αCD163 when stored at 4 °C: the mean radius of CA-LCL-αCD163 increased during prolonged storage at 4 °C (from 70 to 126 nm after 8.5 months), whereas it remained constant for control CA-LCLs. Further, LCL polydispersity (measure of particle size heterogeneity) did not change markedly. Both exhibited high stability in terms of lipid concentration and drug: lipid ratio.

To examine potential leakage of drug from the CA-LCLs, we measured CA concentration before/after ultracentrifugation (UCF; 100,000*g*/30 min) and could not detect CA in the supernatant after UCF (data not shown). This was partly expected due to low solubility of CA. Therefore, we also performed slow centrifugation (400*g*/5 min—which does not pellet liposomes). It is seen that the drug:lipid ratio was unchanged before/after centrifugation for both CA-LCL and CA-LCL-αCD163, whereas free CA was partly pelleted (Fig. 1f)—thus confirming that all CA was still encapsulated in CA-LCL and CA-LCL-αCD163. In complete medium with 10% serum

CA-LCL-αCD163 showed some signs of CA leakage during the first 2 h of incubation, but remained stable from 2 to 24 h.: The drug:lipid ratio was decreased by 32.2% at 24 h, compared to PBS control (Fig. 1g).

Human macrophages with high CD163 expression are targeted by αCD163-modified LCLs

To investigate and visualize CD163-targeted drug delivery to human monocyte-derived macrophages (MDMs) by the humanized monoclonal antibody KN2/NRY, we produced LCLs containing the green fluorescent dye calcein (Cal-LCL) and Cal-LCL-αCD163.

Human MDMs were either untreated, incubated with Cal-LCL, or with Cal-LCL-αCD163. After incubation, cells were prepared for flow cytometry or confocal microscopy as described. As shown in Fig. 2a, b there was a large variation in CD163 expression within cultured MDMs (both intra- and inter-donor). After treatment with non-targeted Cal-LCLs a moderate increase in calcein fluorescence was seen. However, with the CD163-targeted Cal-LCL-αCD163, there was a marked increase in calcein signal (drug uptake) within a fraction of MDMs corresponding to the $CD163^{high}$ cells. The decrease in CD163 signal after treatment with Cal-LCL-αCD163 was likely due to receptor internalization and blocking of the detection antibody. The flow cytometry results were verified in parallel experiments analysed by confocal microscopy, showing low calcein fluorescence in few cells after Cal-LCL treatment, but highly fluorescent cells only in samples treated with Cal-LCL-αCD163 (Fig. 2c).

STAT3-inhibitory effect of CA-LCL-αCD163 in human macrophages

Figure 3a shows histograms of pSTAT3 signal measured by flow cytometry on human MDMs before and after stimulation with IL-10, as well as for MDMs treated with the CA drug formulations before IL-10 stimulation. It is seen that IL-10 activated STAT3, and that this activation was inhibited by both free CA and CA-LCL-αCD163, whereas the non-targeted CA-LCLs did not have inhibitory effect. Figure 3b shows data from three to four independent experiments with MDMs from different donors. Stimulation with IL-10 significantly increased pSTAT3 MFI (~ 2–3-fold increase, $P < 0.001$). The ability of the drug to inhibit STAT3 activation is shown as reduction in relative pSTAT3 signal. Thus, a reduction to 1 implies that drug treatment completely inhibited IL-10-induced activation of STAT3. At 1 μM, only free CA significantly inhibited STAT3 activation ($P < 0.05$). However, at 10 μM both free CA and CA-LCL-αCD163 significantly reduced pSTAT3 MFI levels ($P \leq 0.001$). There was no difference between the effects of free CA and CA-LCL-αCD163 ($P \geq 0.49$). Interestingly, the two donors with largest STAT3-inhibitory effect of CA-LCL-αCD163 had ~ fourfold higher CD163 expression (CD163 MFI ~ 2000) than the two other donors (both MFI ~ 500). See Supplemental Fig. 1 for data validating our flow cytometric assay for detection of activated P-Y705-STAT3.

Toxicity of corosolic acid drug formulations

Viability of human MDMs after 12 or 24 h treatment with free CA, CA-LCL, or CA-LCL-αCD163 at increasing concentrations was determined by CellTiter-Glo luminescence assay (Fig. 3c). Briefly, there was no significant decrease in cell viability after treatment with CA-LCL or CA-LCL-αCD163 at any concentration. In contrast, free CA significantly decreased viability of MDMs at ≥ 30 μM (12 and 24 h, $P < 0.001$). For PBMCs, viability data after 12 h treatment were obtained by flow cytometry (using Live/dead stain). We observed decreased PBMC viability with increasing CA concentration for free CA ($P < 0.0001$) and slightly for CA-LCL-αCD163 ($P = 0.04$), but not for CA-LCLs ($P = 1.0$, see Supplemental Fig. 4b).

CA-LCL-αCD163 inhibits IL-6-induced STAT3 activation in $CD163^{pos}$ monocytes with minor effect in $CD163^{neg}$ lymphocytes

We then investigated the efficiency of CA-LCLs in healthy donor PBMCs containing both $CD163^{neg}$ lymphocytes and $CD163^{pos}$ monocytes. Monocytes express less CD163 than MDMs, and we therefore extended drug treatment time in these experiments (12 h), which were performed as described above for MDMs, except that IL-6 was used to induce STAT3 activation in PBMCs. Only samples with > 75% viable cells were included in the analyses (excluding data for free CA ≥ 30 μM).

Figure 4a shows representative plots from the flow cytometric analyses of untreated PBMCs before and after stimulation with IL-6, as well as with increasing CA concentrations as free CA, CA-LCLs, and CA-LCL-αCD163, respectively. CD163 and pSTAT3 signals decreased with increasing concentrations of CA-LCL-αCD163, whereas this was not the case for non-targeted CA-LCLs.

Figure 4b shows data on STAT3 activation in independent experiments on PBMCs from four different healthy donors. Drug concentration is plotted against fold increase in pSTAT3 signal upon IL-6 stimulation. Stimulation with IL-6 activated STAT3 in roughly half of the $CD163^{neg}$ lymphocytes (MFI ~ twofold over unstimulated), whereas the pSTAT3 signal in $CD163^{pos}$ monocytes was ~ fourfold over the unstimulated level. After treatment with increasing CA concentrations, pSTAT3 levels decreased significantly in $CD163^{pos}$ monocytes for both CA-LCLs

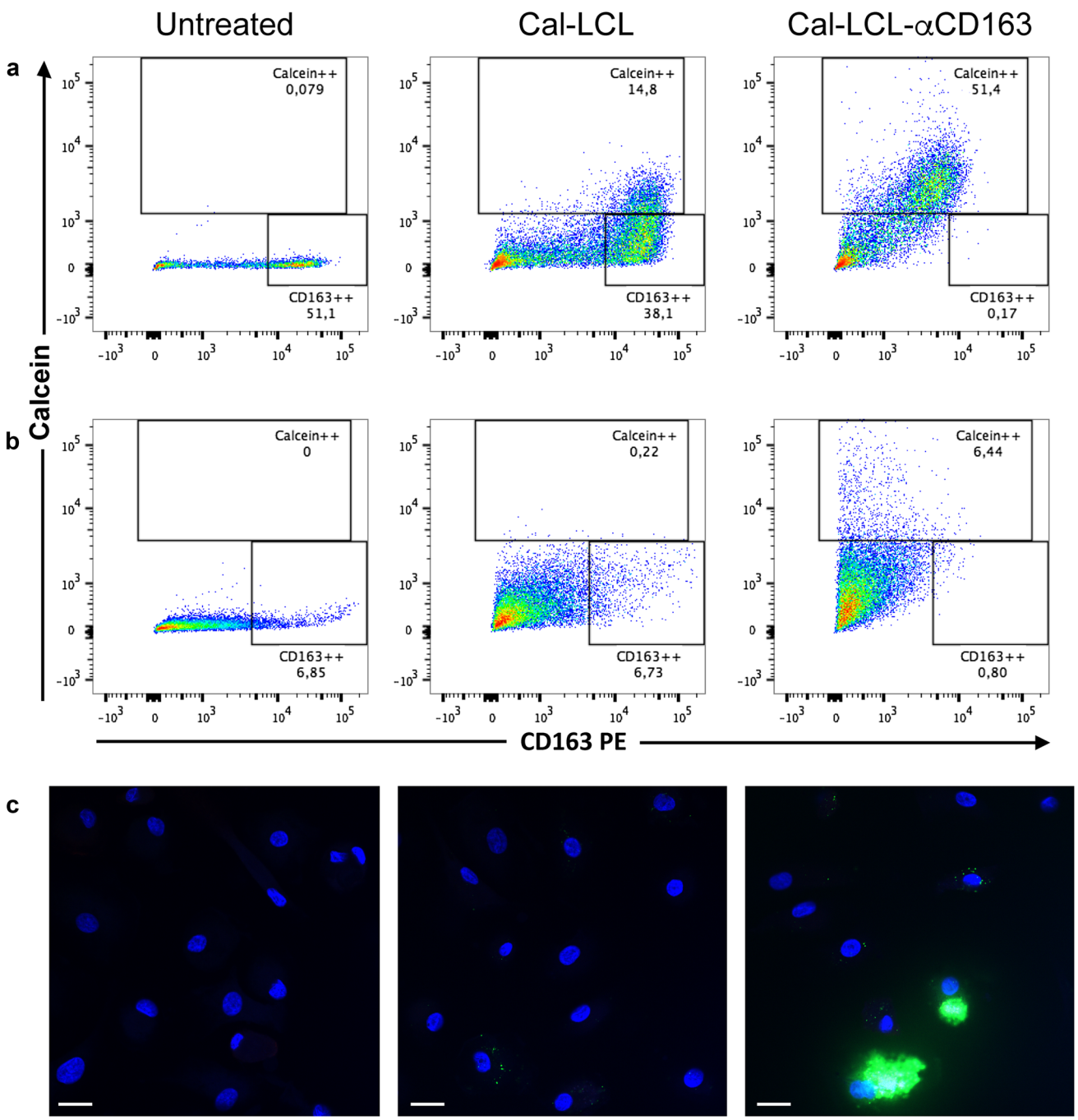

Fig. 2 Targeting of Cal-LCLs to CD163 using humanized monoclonal antibody KN2/NRY. Monocyte-derived macrophages were either untreated (left column), treated with non-targeted calcein-containing LCLs (Cal-LCL, middle), or with targeted Cal-LCL-αCD163 (right) at 20 μM lipid for 90 min at 37 °C. **a, b** Flow cytometry dot plots of CD163 vs. calcein signal showing data from experiments on MDMs from two different donors (**a, b**, respectively) having different CD163 expression pattern. **c** Representative confocal images of the same cells as used for flow cytometry in b (white bars indicate 20 μm). It is seen that cultured MDMs from the two donors have highly variable CD163 expression patterns (**a, b**), with ~51% and ~7% of the cells having very high expression (left). CD163 signal was not affected by treatment with Cal-LCL (middle). Upon treatment with CD163-targeted Cal-LCL-αCD163 (right), the CD163 expression decreased (due to receptor internalization and blocking of the detection mAb), whereas the calcein signal was markedly increased in a fraction of cells corresponding to CD163++ cells (~51% and ~7%). The results are representative for experiments performed with MDMs from three different healthy donors

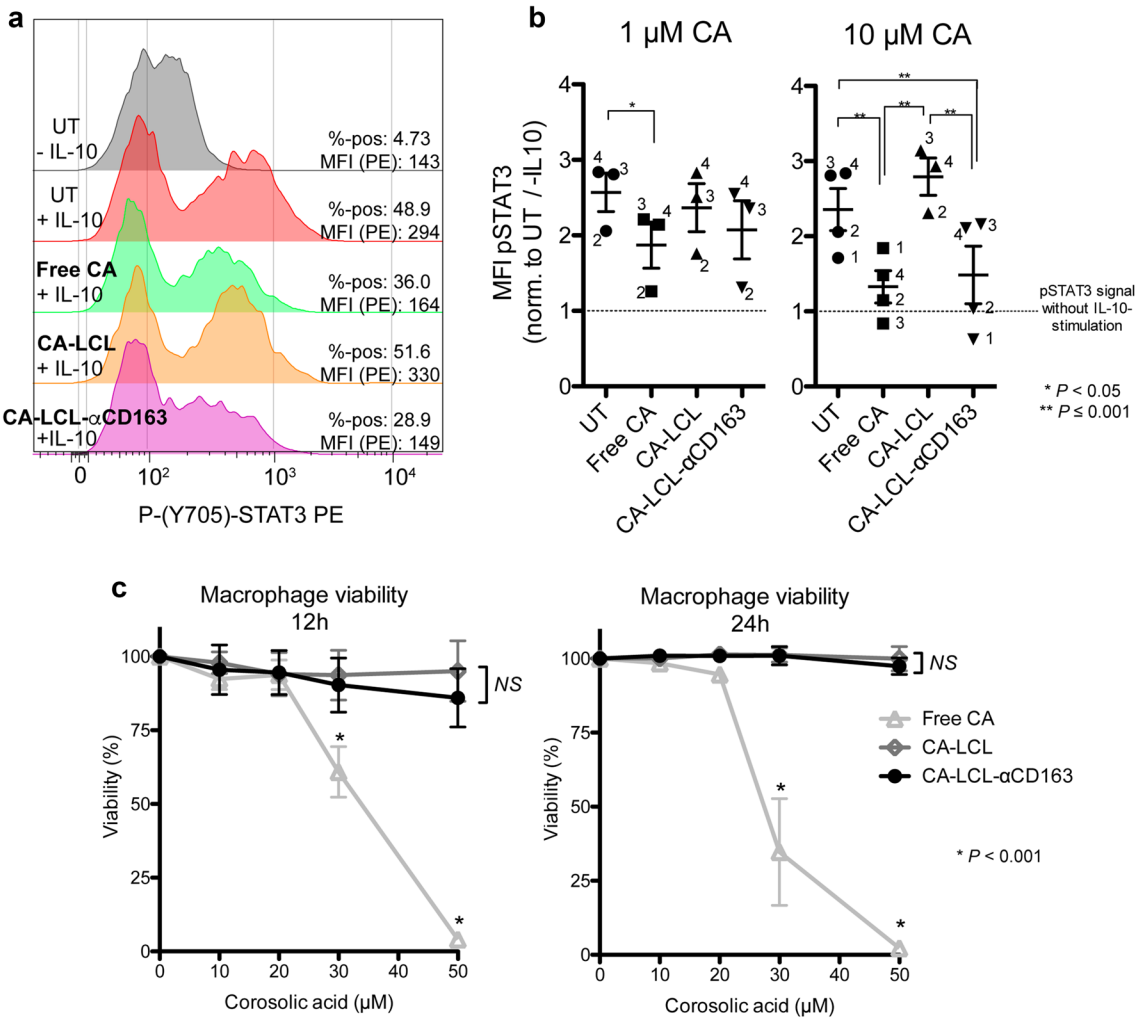

Fig. 3 Targeted STAT3-inhibition in MDMs by CA-LCL-αCD163. Monocyte-derived macrophages were first treated for 2 h with free CA, CA-LCL, or CA-LCL-αCD163 (1 or 10 μM CA). Cells were washed, rested in fresh medium for 1 h, and were then stimulated with 50 ng/mL IL-10 for 15 min to induce STAT3 activation. **a** Representative data from one donor. STAT3 activation level is shown on the *X*-axis. The %-positive cells upon stimulation with IL-10 (gated on control stained with Live/dead only), as well as MFI values for the whole population are shown. **b** Data from four independent experiments (MDMs from different donors). Numbering of each data point represents experiment/donor number. Results are pSTAT3 MFI (gated on all live/single cells) normalized to the UT sample without IL-10 stimulation. Thus, the level of 2–3 in UT samples represents the fold increase in pSTAT3 MFI upon IL-10 stimulation. On drug treatment, a reduction in pSTAT3 MFI to the level without IL-10 stimulation equals a reduction to 1 (dotted line). The two donors (1 and 2) with the highest STAT3-inhibitory effect of CA-LCL-αCD163 had CD163 FITC MFI ~ 2000, corresponding to fourfold higher CD163 expression than the two additional donors (MFI ~ 500). See Supplemental Fig. 3 for flow cytometry data from all four donors. **c** Viability data from four independent experiments on MDMs. Drugs (free CA, CA-LCL, or CA-LCL-αCD163) were added in stated final concentrations of CA. Medium (UT) served as control. After 12 or 24 h incubation, cell viability was assessed using CellTiter-Glo luminescence assay. Results were normalized to UT signals, thus UT wells were set to 100% viability. Increased drug concentration of free CA decreased MDM viability ($P < 0.001$), whereas CA-LCL and CA-LCL-αCD163 did not. Asterisks indicate individual concentrations with significantly decreased viability compared to UT. See Supplemental Fig. 4 for viability data on PBMCs and stromal cell line HS-27

($P = 0.02$) and CA-LCL-αCD163 ($P < 0.0001$). However, CA-LCL-αCD163 was more effective than CA-LCL at both 30 and 50 μM CA ($P \leq 0.05$). Importantly, the effect of CA-LCLs on $CD163^{neg}$ lymphocytes was minor, and there was no difference between the effects of CA-LCL-αCD163 and CA-LCLs ($P > 0.2$).

CA-LCL-αCD163 inhibits IL-10-induced gene expression in human MDMs

The results described above show that STAT3 activation by Y705-phosphorylation was inhibited specifically within CD163 expressing cells. We then investigated whether this

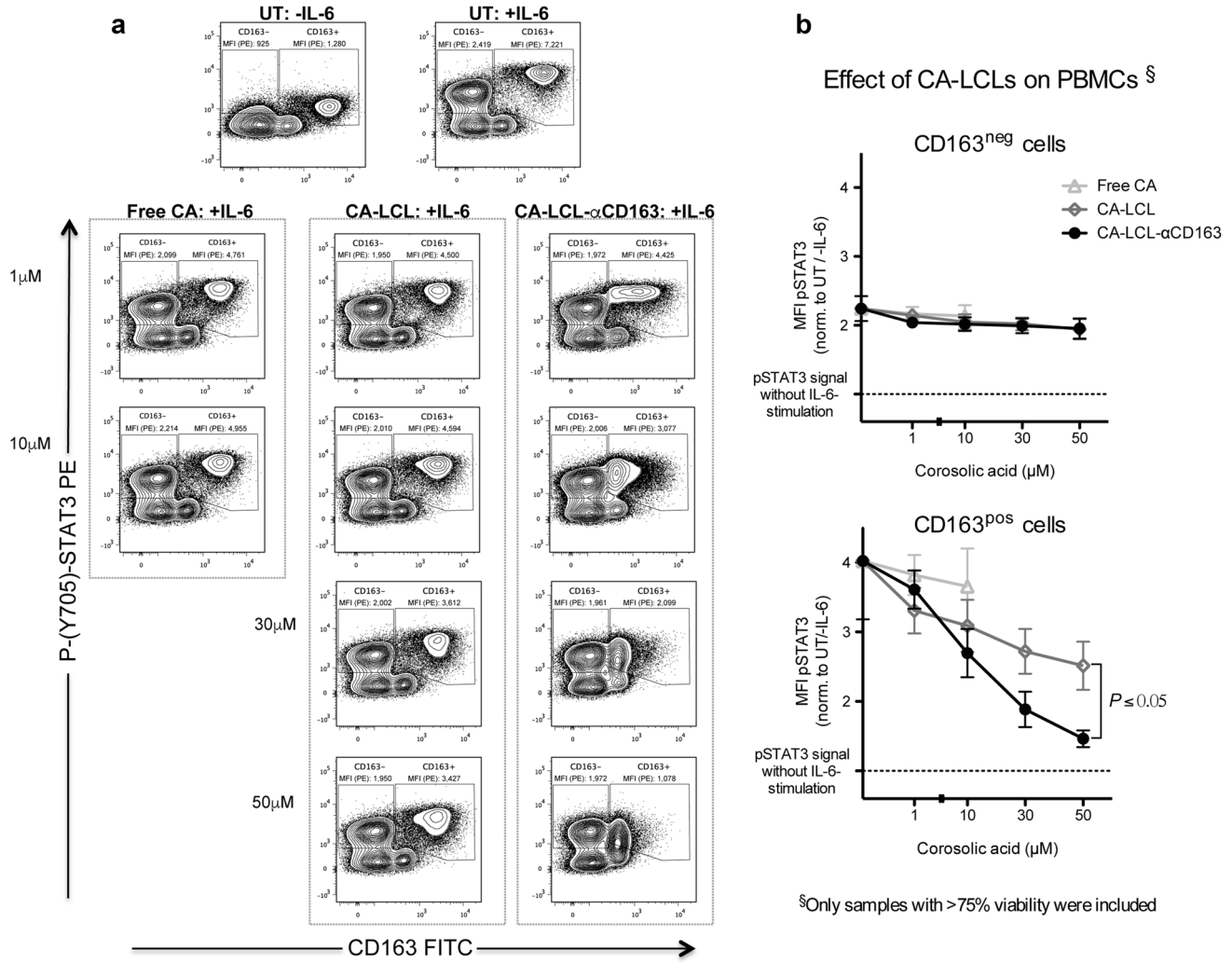

Fig. 4 CA-LCL-αCD163 inhibits STAT3 activity specifically in $CD163^{pos}$ PBMCs. Human PBMCs were treated for 12 h with free CA, non-targeted CA-LCLs, or CA-LCL-αCD163 (1–50 μM CA). Cells were washed, rested in fresh medium for 1 h, and were then stimulated with 50 ng/mL IL-6 for 15 min to induce STAT3 activation by phosphorylation of Tyr 705 (pSTAT3). Only samples with viability > 75% were included, thus excluding data on free CA ≥ 30 μM (see Supplemental Fig. 4). **a** Representative data from flow cytometric analysis of PBMCs: CD163 vs. P-(Y705)-STAT3. The top row shows plots of untreated PBMCs (UT) with/without IL-6 stimulation. Lower rows show PBMCs treated with free CA (left), non-targeted CA-LCLs (middle), and CA-LCL-αCD163 (right) at increasing CA concentrations. Apparently, for CA-LCL-αCD163, increasing drug concentrations decreased CD163 signal with a parallel decrease in pSTAT3 signal. With 50 μM CA the STAT3 activity was almost completely inhibited by CA-LCL-αCD163 within the $CD163^{pos}$ subset of PBMCs, whereas there was minor effect in $CD163^{neg}$ cells. With non-targeted CA-LCLs this effect was not seen. **b** Data on pSTAT3 levels after drug treatment and IL-6 stimulation of PBMCs from different donors ($n = 4$). $CD163^{neg}$ (top) and $CD163^{pos}$ (bottom) populations were gated as shown in **a**. The *x*-axis shows CA concentration within the medium. The *y*-axis shows fold-changes: the pSTAT3 MFI of drug-treated and IL-6-stimulated samples was normalized to the MFI of UT cells not stimulated with IL-6. Thus, a value of 1 (dotted line) indicates that the treatment completely inhibited activation of STAT3. It is seen that in $CD163^{pos}$ monocytes (bottom) CA-LCL-αCD163 inhibited IL-6-induced STAT3 activation more effectively than CA-LCLs at both 30 and 50 μM ($P \leq 0.05$), whereas this was not the case in $CD163^{neg}$ lymphocytes (top, $P > 0.2$)

inhibition also modulated the expression of STAT3-regulated genes. As described, IL-10 induces mRNA synthesis of CD163 as well as IL-10 itself in human macrophages. We therefore investigated whether CA-LCLs would inhibit IL-10-induced synthesis of mRNA encoding the M2-markers CD163 and IL-10. Furthermore, we analysed mRNA levels of pro-inflammatory TNFα after treatment.

In Fig. 5, it is seen that IL-10 stimulation increased expression of both CD163 ($P = 0.002$) and IL-10 ($P = 0.02$) mRNA, and slightly decreased levels of TNFα (though not significant, $P = 0.09$). Due to toxicity, concentrations ≥ 30 μM free CA were excluded. Non-targeted CA-LCLs did not affect gene expression (all $P > 0.5$). However, CA-LCL-αCD163 decreased IL-10 gene expression to the

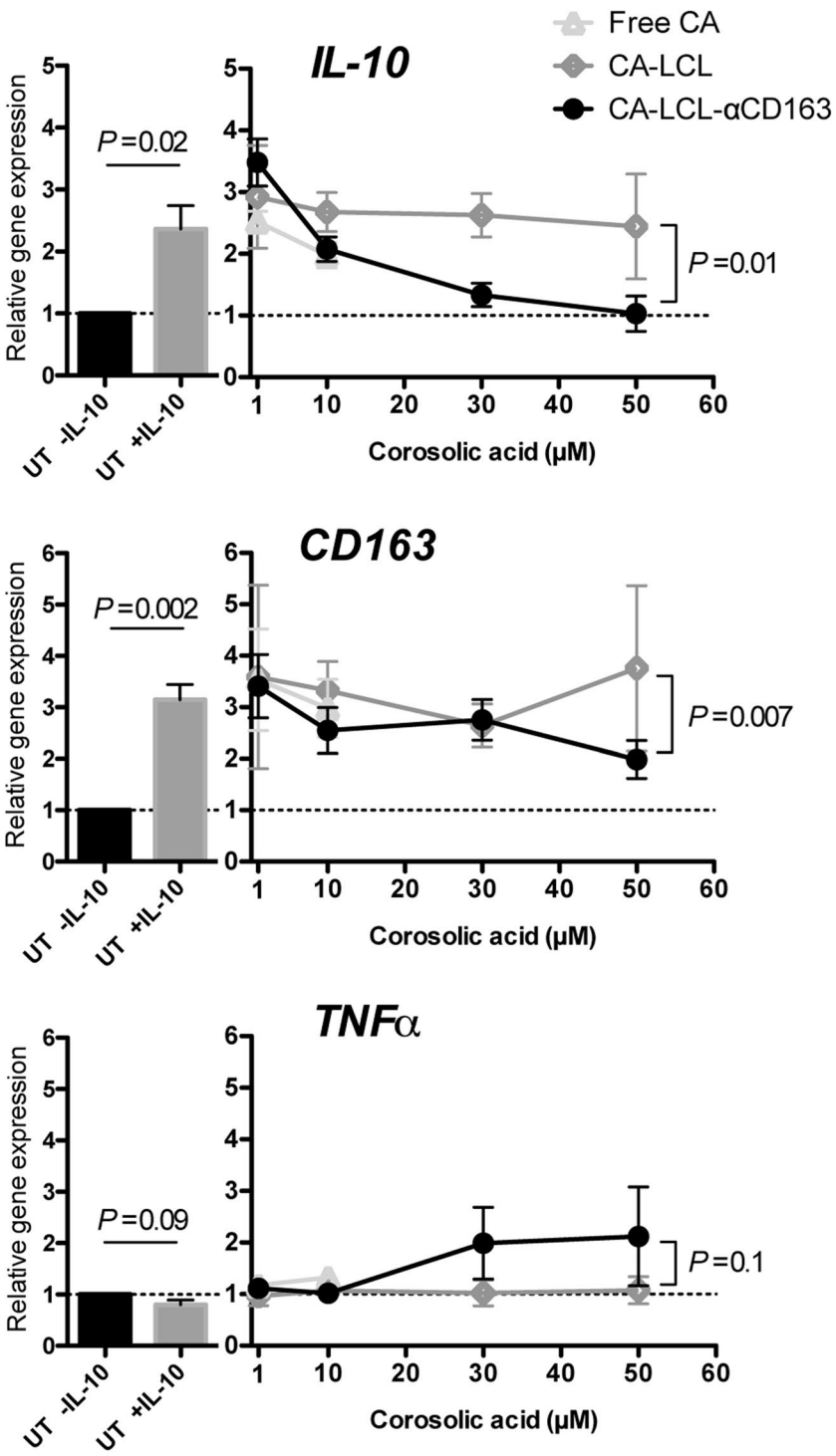

Fig. 5 CD163-targeted CA-LCLs modulate IL-10-induced gene expression in MDMs. Human MDMs ($n=5$ donors) were treated with increasing concentrations of free CA, CA-LCLs, or CA-LCL-αCD163, or were left untreated (UT, medium control) for 12 h, with simultaneous stimulation with 50 ng/mL IL-10. After 12 h, cells were lysed and RNA purified, reverse transcribed, and used for qPCR. Gene expression results were normalized to the UT samples not stimulated with IL-10, and thus represent fold change upon IL-10 stimulation with or without drug treatment. Due to toxicity, data for concentrations ≥ 30 μM free CA were excluded (see Fig. 3). In the left part, it is seen that IL-10 stimulation of UT MDMs increased mRNA levels of both IL-10 itself ($P=0.02$) and CD163 ($P=0.002$), whereas TNFα was slightly decreased (borderline significant). To the right is shown fold change in mRNA levels upon IL-10 stimulation with simultaneous drug treatment (1–50 μM final CA concentration, *X*-axis). The *Y*-axis shows fold-changes in mRNA levels as described. Thus, a value of 1 (dotted line) indicates that the treatment was able to completely inhibit IL-10-induced gene expression. Non-targeted CA-LCLs had no significant effect on mRNA levels (all $P>0.5$). CA-LCL-αCD163 was significantly more effective than non-targeted CA-LCLs in decreasing IL-10 ($P=0.01$) and CD163 ($P=0.007$), and induced slight non-significant increase in TNFα expression ($P=0.1$)

unstimulated level ($P=0.002$), slightly inhibited CD163 expression (at 50 μM, $P=0.08$), and increased expression of TNFα ($P<0.05$). Furthermore, the ability of CA-LCL-αCD163 to modulate IL-10-induced gene expression was significantly greater than that of non-targeted CA-LCLs for IL-10 ($P=0.01$) and CD163 ($P=0.007$), but not statistically significant for TNFα ($P=0.1$).

CA-LCL-αCD163 induces pro-inflammatory cytokine production in human MDMs

The gene expression analyses described above indicated an M1-like reprogramming effect of CA-LCL-αCD163 on MDMs. To further investigate such reprogramming, we measured levels of pro-inflammatory (M1-related) cytokines

in the medium collected from the gene expression experiments ($n=5$). Figure 6 shows that IL-10 stimulation alone (no drug treatment, left figure parts) slightly induced production of IL-2 and IL-12 (both $P<0.05$). Upon drug treatment, neither free CA nor CA-LCLs showed statistically significant effect on cytokine production (all $P>0.7$). However, increasing concentrations of CA-LCL-αCD163 significantly induced production of IFNγ ($P=0.008$), TNFα ($P<0.0001$), IL-2 ($P=0.02$), and IL-12 ($P=0.002$). Furthermore, the effect of CA-LCL-αCD163 was also significantly larger than non-targeted control CA-LCLs (all $P<0.01$, Fig. 6).

Discussion

Tumor-associated macrophages have been a major focus in cancer research during recent years, and several endeavours have been made into targeting the cancer-promoting TAMs to improve anti-cancer therapy [4, 12, 16]. Inhibition of CSF-1 signalling has shown promising results, likely due to depletion of TAMs. However, one study indicated that the anti-cancer effect was mediated by reprogramming of TAMs towards a pro-inflammatory (M1-like) phenotype [14, 16], which may have greater effect than simple depletion [12].

Notably, the transcription factor STAT3 is an attractive target for novel anti-cancer therapy [17–19], and data have indicated that STAT3 inhibition within TAMs may reprogram these cells and induce anti-tumor immunity [4, 19, 24, 25, 27]. In one report, STAT3 inhibition (by genetic ablation) specifically within CD68 expressing TAMs reduced tumor cell proliferation and motility, decreased angiogenesis and metastasis, and prolonged survival of mice in a breast cancer model [28]. However, no previous reports have shown data on a STAT3-inhibitory drug that can be targeted specifically to TAMs.

One efficient gateway for targeting and reprogramming TAMs may be the hemoglobin–haptoglobin scavenger receptor CD163 [39]. The endocytic CD163 is overexpressed in human TAMs [9, 30, 35], and tumor infiltration by CD163^{pos}

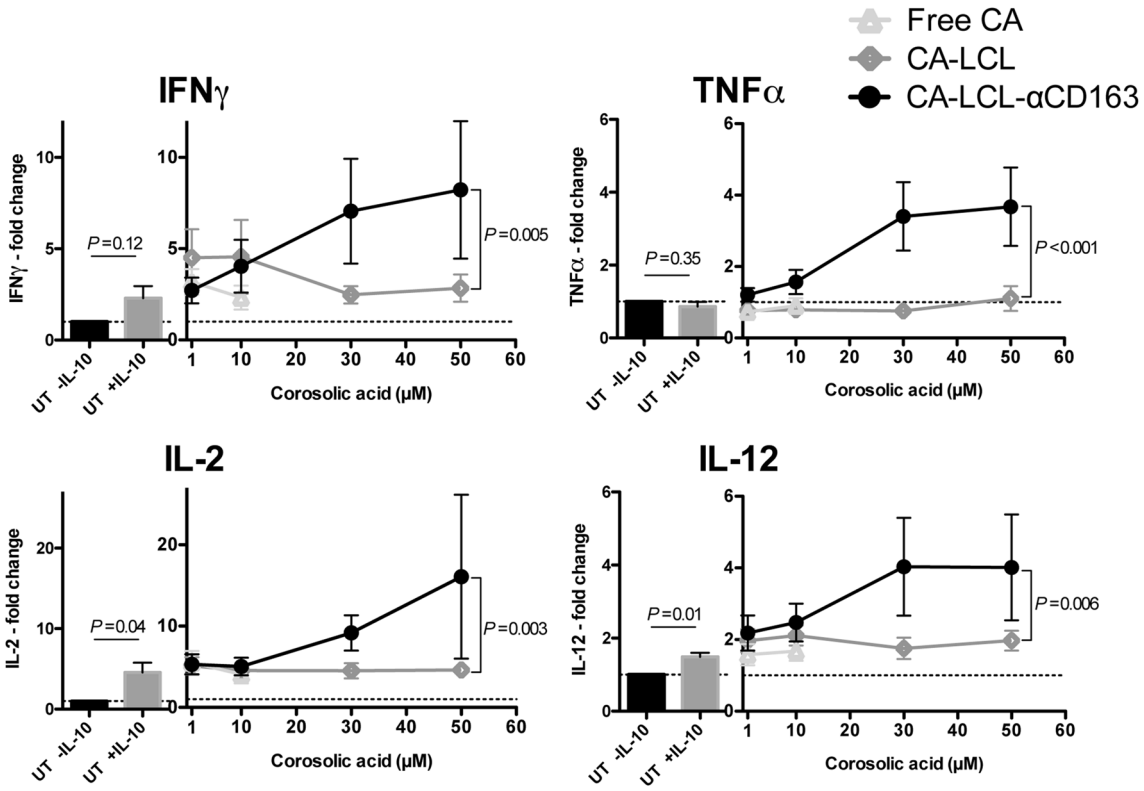

Fig. 6 CD163-targeted CA-LCLs induce M1-like cytokine profile in MDMs. Levels of pro-inflammatory cytokines IFNγ, TNFα, IL-2 and IL-12 were measured in culture medium collected after 12 h IL-10 stimulation of MDMs with/without drug treatment (free CA, CA-LCLs, or CA-LCL-αCD163) as described for the gene expression data (Fig. 5). Due to toxicity, concentrations of ≥ 30 μM free CA were excluded (see Fig. 3). It is seen that IL-10 stimulation (without drug treatment) induced minor production of IL-2 and IL-12 (left figure parts). Further, increasing the concentration of CA-LCL-αCD163 induced significant production of the four cytokines. Shown *P* values represent tested differences between control CA-LCLs and CA-LCL-αCD163 at 50 μM. Results were normalized to the medium control samples (UT) not stimulated with IL-10. A single TNFα outlier was removed from the CA-LCL 30 μM group, which did not affect the overall results of the statistical analyses

TAMs is associated with poor outcome in several human malignancies [5, 7, 31].

Here, we present the first data on development of a novel CD163-targeted STAT3-inhibitory drug, consisting of corosolic acid-containing long-circulating liposomes (CA-LCLs) targeted to $CD163^{pos}$ cells using a humanized anti-CD163 antibody (αCD163). Thus, the drug targets the (monocyte–macrophage lineage-specific) receptor CD163, which takes up the drug by endocytosis. We show that CA could be effectively remote-loaded into LCLs, and the resulting CA-LCLs were stable, with no drug leakage, when stored at 4 °C for several months. However, in complete medium we saw signs of moderate drug leakage, indicating that drug effects may be enhanced by further chemical modifications. Such improvements should be undertaken before future in vivo experiments. The αCD163-modified CA-LCLs showed sign of liposome fusion (increased size) during prolonged storage (months). The biochemical background for this is not known, but it should be taken into account in future in vivo studies, since endothelial pore size may vary within different tissues [45] and nanoparticle size might impact uptake by endocytosis [46].

Since we have previously shown only slight increase in drug uptake with IgG-modified LCLs, compared to non-modified LCLs [39], we used non-modified CA-LCLs as controls for determining non-specific drug uptake. A limitation of the present study is that all results are from in vitro experiments. Thus, experiments in animal models of cancer are needed to evaluate the effect of CA-LCL-αCD163 in malignant diseases. However, the goal of the present study was to provide proof of principle, and the results encourage further studies.

A previous study showed that free CA induced apoptosis in a human glioma cells in vitro, whereas viability of human macrophages and lymphocytes was not affected [37]. In another study, results indicated an immune-activating anti-tumor effect of CA in vivo, which was synergistic in combination with cytostatic treatment [38]. In the present study, cell viability decreased on treatment with free CA ≥ 30 µM, whereas CA-LCLs had no or minor impact on cell viability. The reason for this difference is not known and should be investigated further.

We tracked uptake of calcein-loaded LCLs (Cal-LCLs) in human monocyte-derived macrophages (MDMs) by flow cytometry and confocal microscopy. This showed high uptake of CD163-targeted Cal-LCLs in $CD163^{high}$ cells, thus confirming our previous findings in CD163-transfected HEK293 cells [39] in cultured human MDMs. The decrease in CD163 expression after treatment with CD163-targeted LCLs in the present study (due to receptor internalization/blocking of detection mAb) was not seen in the previous study, likely due to a 24 h resting phase after treatment with Cal-LCL-αCD163 [39].

In human MDMs, CA-LCL-αCD163 inhibited STAT3 activation (inhibited Y705 phosphorylation). Further, within human PBMCs, CA-LCL-αCD163 effectively inhibited STAT3 activation in $CD163^{pos}$ monocytes, with minor effect in $CD163^{neg}$ lymphocytes—confirming the CD163-specific targeting of the drug. Some uptake of non-targeted CA-LCLs in monocytes was indicated by the results, which was expected from previous studies [39, 40]. The larger effect of non-targeted CA-LCLs on monocytes compared to MDMs was likely due to longer treatment time (12 h vs. 2 h). However, the CD163-targeted CA-LCL-αCD163 showed significantly higher STAT3-inhibitory effect than non-targeted CA-LCLs. Importantly, CA-LCL-αCD163 not only inhibited STAT3 activation on protein level, but also modulated downstream gene expression, indicative of a reprogramming of MDMs towards an M1-like phenotype. These results were verified by induction of pro-inflammatory cytokine production (IFNγ, TNFα, IL-2 and IL-12) by CA-LCL-αCD163. Thus, our data are in line with previous studies showing M1-like reprogramming of TAMs by STAT3 inhibition [24, 25], which was associated with anti-tumor effects [19, 28].

Immune-activating anti-cancer therapies, including STAT3 inhibition, have shown risk of autoimmune complications, especially colitis [4, 26, 47]. This highlights the need for development of approaches with specific targeting of cells important for establishing the tumor-promoting microenvironment. Since TAMs are present in large numbers within human tumors (up to 50% of cells in some tumors) [30], and since TAMs perform multiple tumor-promoting functions as described above, these cells may be ideal targets for novel immune-activating treatments [4, 12]. Furthermore, using a liposome-based approach may lead to passive drug accumulation within tumors, owing to the EPR effect. However, the EPR effect in humans is not well investigated, and its magnitude is variable [45], which may further emphasize the importance of active CD163-targeting.

In conclusion, even though several reports have indicated striking effects of modulating STAT3-signalling in immune cells (especially in myeloid cells), to our knowledge, this is the first report to show development of a STAT3-inhibitory drug that can be targeted specifically to human $CD163^{pos}$ cells (which includes TAMs). Such targeting may increase the effects, and decrease side effects, of future STAT3-inhibitory anti-cancer therapy. The present study provides proof of principle for a pro-inflammatory reprogramming effect of our CD163-targeted STAT3-inhibitory drug in vitro, but the lack of in vivo data is a limitation. Thus, experiments in animal models are highly warranted, and should be pursued in future studies.

Acknowledgements All flow cytometry experiments were performed using the LSR Fortessa flow cytometer at the FACS Core Facility, Aarhus University, Denmark. The authors wish to thank Zane Binate,

Lene Dabelstein, Helle Ryom, and Christina Sønderskov for excellent technical assistance.

Author contributions Conception and design: MNA, AE, JHG, SKM, MH, HJM. Acquisition of data: MNA, AE, LCH. Analysis and interpretation of data: MNA, AE, MH, HJM. Drafting the article: MNA. All authors revised the manuscript critically, and approved the version to be published.

Funding Institutional funding: Department of Clinical Biochemistry, Aarhus University Hospital, Denmark; and the Faculty of Health, Aarhus University, Denmark. Funding of Morten N Andersen: The Danish Cancer Research Foundation; The Cancer Foundation (Denmark); The Memorial Foundation of Eva and Henry Frænkel; and The Memorial Foundation of Max and Inger Wørzner. Funding of Anders Etzerodt: The Novo Nordisk Foundation.

Compliance with ethical standards

Conflict of interest Jonas H. Graversen, Søren K. Moestrup, and Holger J. Møller are minority shareholders in Affinicon ApS, which holds IP protecting the use of CD163 drug targeting. The other authors declare no conflict of interest.

Ethical approval and ethical standards Buffy coats (residual product from blood processing) were collected anonymously from volunteer donors during routine blood donation at the blood bank, Department of Clinical Immunology, Aarhus University Hospital, Denmark (project number 0094). Volunteers gave informed written consent before blood donation. According to Danish law, this use of anonymized buffy coats does not require separate ethical approval.

References

1. Hanahan D, Weinberg RA (2011) Hallmarks of cancer: the next generation. Cell 144:646–674. https://doi.org/10.1016/j.cell.2011.02.013
2. Gibney GT, Weiner LM, Atkins MB (2016) Predictive biomarkers for checkpoint inhibitor-based immunotherapy. Lancet Oncol 17:e542–e551. https://doi.org/10.1016/S1470-2045(16)30406-5
3. Noy R, Pollard JW (2014) Tumor-associated macrophages: from mechanisms to therapy. Immunity 41:49–61. https://doi.org/10.1016/j.immuni.2014.06.010
4. Komohara Y, Fujiwara Y, Ohnishi K, Takeya M (2016) Tumor-associated macrophages: potential therapeutic targets for anti-cancer therapy. Adv Drug Deliv Rev 99:180–185. https://doi.org/10.1016/j.addr.2015.11.009
5. Zhang Q-W, Liu L, Gong C-Y et al (2012) Prognostic significance of tumor-associated macrophages in solid tumor: a meta-analysis of the literature. PLoS One 7:e50946. https://doi.org/10.1371/journal.pone.0050946
6. Komohara Y, Niino D, Ohnishi K et al (2015) Role of tumor-associated macrophages in hematological malignancies. Pathol Int 65:170–176. https://doi.org/10.1111/pin.12259
7. Yang M, McKay D, Pollard JW, Lewis CE (2018) Diverse functions of macrophages in different tumor microenvironments. Cancer Res 78:5492–5503. https://doi.org/10.1158/0008-5472.CAN-18-1367
8. Porcheray F, Viaud S, Rimaniol A-C et al (2005) Macrophage activation switching: an asset for the resolution of inflammation. Clin Exp Immunol 142:481–489. https://doi.org/10.1111/j.1365-2249.2005.02934.x
9. Biswas SK, Mantovani A (2010) Macrophage plasticity and interaction with lymphocyte subsets: cancer as a paradigm. Nat Immunol 11:889–896. https://doi.org/10.1038/ni.1937
10. Hagemann T, Lawrence T, McNeish I et al (2008) "Re-educating" tumor-associated macrophages by targeting NF-κB. J Exp Med 205:1261–1268. https://doi.org/10.1136/ard.59.suppl_1.i54
11. Duluc D, Corvaisier M, Blanchard S et al (2009) Interferon-gamma reverses the immunosuppressive and protumoral properties and prevents the generation of human tumor-associated macrophages. Int J Cancer 125:367–373. https://doi.org/10.1002/ijc.24401
12. Awad RM, De Vlaeminck Y, Maebe J et al (2018) Turn back the time: targeting tumor infiltrating myeloid cells to revert cancer progression. Front Immunol 9:1977. https://doi.org/10.3389/fimmu.2018.01977
13. DeNardo DG, Brennan DJ, Rexhepaj E et al (2011) Leukocyte complexity predicts breast cancer survival and functionally regulates response to chemotherapy. Cancer Discov 1:54–67. https://doi.org/10.1158/2159-8274.CD-10-0028
14. Pyonteck SM, Akkari L, Schuhmacher AJ et al (2013) CSF-1R inhibition alters macrophage polarization and blocks glioma progression. Nat Med 19:1264–1272. https://doi.org/10.1038/nm.3337
15. Ries CH, Cannarile MA, Hoves S et al (2014) Targeting tumor-associated macrophages with anti-CSF-1R antibody reveals a strategy for cancer therapy. Cancer Cell 25:846–859. https://doi.org/10.1016/j.ccr.2014.05.016
16. Quail DF, Joyce JA (2017) Molecular pathways: deciphering mechanisms of resistance to macrophage-targeted therapies. Clin Cancer Res 23:876–884. https://doi.org/10.1158/1078-0432.CCR-16-0133
17. Yu H, Pardoll D, Jove R (2009) STATs in cancer inflammation and immunity: a leading role for STAT3. Nat Rev Cancer 9:798–809. https://doi.org/10.1038/nrc2734
18. Yu H, Lee H, Herrmann A et al (2014) Revisiting STAT3 signalling in cancer: new and unexpected biological functions. Nat Rev Cancer 14:736–746. https://doi.org/10.1038/nrc3818
19. Su Y-L, Banerjee S, White SV, Kortylewski M (2018) STAT3 in tumor-associated myeloid cells: multitasking to disrupt immunity. Int J Mol Sci. https://doi.org/10.3390/ijms19061803
20. Mukherjee S, Hussaini R, White R et al (2018) TriCurin, a synergistic formulation of curcumin, resveratrol, and epicatechin gallate, repolarizes tumor-associated macrophages and triggers an immune response to cause suppression of HPV+ tumors. Cancer Immunol Immunother 67:761–774. https://doi.org/10.1007/s00262-018-2130-3
21. Mano Y, Aishima S, Fujita N et al (2013) Tumor-associated macrophage promotes tumor progression via STAT3 signaling in hepatocellular carcinoma. Pathobiology 80:146–154. https://doi.org/10.1159/000346196
22. Chai EZP, Shanmugam MK, Arfuso F et al (2016) Targeting transcription factor STAT3 for cancer prevention and therapy. Pharmacol Ther 162:86–97. https://doi.org/10.1016/j.pharmthera.2015.10.004
23. Cheng F, Cheng F, Wang H-W et al (2003) A critical role for Stat3 signaling in immune tolerance. Immunity 19:425–436. https://doi.org/10.1016/S1074-7613(03)00232-2
24. Sun Z, Yao Z, Liu S et al (2006) An oligonucleotide decoy for Stat3 activates the immune response of macrophages to breast cancer. Immunobiology 211:199–209. https://doi.org/10.1016/j.imbio.2005.11.004
25. Zhang L, Alizadeh D, Van Handel M et al (2009) Stat3 inhibition activates tumor macrophages and abrogates glioma growth in mice. Glia 57:1458–1467. https://doi.org/10.1002/glia.20863
26. Kortylewski M, Kujawski M, Wang T et al (2005) Inhibiting Stat3 signaling in the hematopoietic system elicits multicomponent

antitumor immunity. Nat Med 11:1314–1321. https://doi.org/10.1038/nm1325
27. Herrmann A, Kortylewski M, Kujawski M et al (2010) Targeting Stat3 in the myeloid compartment drastically improves the in vivo antitumor functions of adoptively transferred T cells. Cancer Res 70:7455–7464. https://doi.org/10.1158/0008-5472.CAN-10-0736
28. Dang W, Tang H, Cao H et al (2015) Strategy of STAT3β cell-specific expression in macrophages exhibits antitumor effects on mouse breast cancer. Gene Ther 22:977–983. https://doi.org/10.1038/gt.2015.70
29. Giurisato E, Xu Q, Lonardi S et al (2018) Myeloid ERK5 deficiency suppresses tumor growth by blocking protumor macrophage polarization via STAT3 inhibition. Proc Natl Acad Sci 115:E2801–E2810. https://doi.org/10.1073/pnas.1707929115
30. Solinas G, Germano G, Mantovani A, Allavena P (2009) Tumor-associated macrophages (TAM) as major players of the cancer-related inflammation. J Leukoc Biol 86:1065–1073. https://doi.org/10.1189/jlb.0609385
31. Komohara Y, Jinushi M, Takeya M (2014) Clinical significance of macrophage heterogeneity in human malignant tumors. Cancer Sci 105:1–8. https://doi.org/10.1111/cas.12314
32. Jensen TO, Schmidt H, Møller HJ et al (2009) Macrophage markers in serum and tumor have prognostic impact in american joint committee on cancer stage I/II melanoma. J Clin Oncol 27:3330–3337. https://doi.org/10.1200/JCO.2008.19.9919
33. Wada N, Zaki MAA, Hori Y et al (2012) Tumour-associated macrophages in diffuse large B-cell lymphoma: a study of the Osaka Lymphoma Study Group. Histopathology 60:313–319. https://doi.org/10.1111/j.1365-2559.2011.04096.x
34. Staples KJ, Smallie T, Williams LM et al (2007) IL-10 induces IL-10 in primary human monocyte-derived macrophages via the transcription factor Stat3. J Immunol 178:4779–4785. https://doi.org/10.4049/jimmunol.178.8.4779
35. Hasita H, Komohara Y, Okabe H et al (2010) Significance of alternatively activated macrophages in patients with intrahepatic cholangiocarcinoma. Cancer Sci 101:1913–1919. https://doi.org/10.1111/j.1349-7006.2010.01614.x
36. Komohara Y, Komohara Y, Hasita H et al (2011) Macrophage infiltration and its prognostic relevance in clear cell renal cell carcinoma. Cancer Sci 102:1424–1431. https://doi.org/10.1111/j.1349-7006.2011.01945.x
37. Fujiwara Y, Komohara Y, Ikeda T, Takeya M (2010) Corosolic acid inhibits glioblastoma cell proliferation by suppressing the activation of signal transducer and activator of transcription-3 and nuclear factor-kappa B in tumor cells and tumor-associated macrophages. Cancer Sci 102:206–211. https://doi.org/10.1111/j.1349-7006.2010.01772.x
38. Horlad H, Fujiwara Y, Takemura K et al (2013) Corosolic acid impairs tumor development and lung metastasis by inhibiting the immunosuppressive activity of myeloid-derived suppressor cells. Mol Nutr Food Res 57:1046–1054. https://doi.org/10.1002/mnfr.201200610
39. Etzerodt A, Maniecki MB, Graversen JH et al (2012) Efficient intracellular drug-targeting of macrophages using stealth liposomes directed to the hemoglobin scavenger receptor CD163. J Control Release 160:72–80. https://doi.org/10.1016/j.jconrel.2012.01.034
40. Prabhakar U, Maeda H, Jain RK et al (2013) Challenges and key considerations of the enhanced permeability and retention effect for nanomedicine drug delivery in oncology. Cancer Res 73(8):2412–2417. https://doi.org/10.1158/0008-5472.CAN-12-4561
41. Ngoune R, Peters A, Elverfeldt von D et al (2016) Accumulating nanoparticles by EPR: A route of no return. J Control Release 238:58–70. https://doi.org/10.1016/j.jconrel.2016.07.028
42. Clerc S, Barenholz Y (1995) Loading of amphipathic weak acids into liposomes in response to transmembrane calcium acetate gradients. Biochim Biophys Acta 1240:257–265. https://doi.org/10.1016/0005-2736(95)00214-6
43. Granfeldt A, Hvas CL, Graversen JH et al (2013) Targeting dexamethasone to macrophages in a porcine endotoxemic model. Crit Care Med 41:e309–e318. https://doi.org/10.1097/CCM.0b013e31828a45ef
44. Andersen MN, Al-Karradi SNH, Kragstrup TW, Hokland M (2016) Elimination of erroneous results in flow cytometry caused by antibody binding to Fc receptors on human monocytes and macrophages. Cytom A 89:1001–1009. https://doi.org/10.1002/cyto.a.22995
45. Danhier F (2016) To exploit the tumor microenvironment: Since the EPR effect fails in the clinic, what is the future of nanomedicine? J Control Release 244:108–121. https://doi.org/10.1016/j.jconrel.2016.11.015
46. Oh N, Park JH (2014) Endocytosis and exocytosis of nanoparticles in mammalian cells. IJN 9(Suppl 1):51–63. https://doi.org/10.2147/IJN.S26592
47. Welte T, Zhang SSM, Wang T et al (2003) STAT3 deletion during hematopoiesis causes Crohn's disease-like pathogenesis and lethality: a critical role of STAT3 in innate immunity. Proc Natl Acad Sci USA 100:1879–1884. https://doi.org/10.1073/pnas.0237137100